A Modified Synthetic Aperture Focussing Technique Utilising the Spatial Impulse Response of the Ultrasound Transducer

Stephen A. MOSEY [1], Peter C. CHARLTON [1], Ian WELLS [1]

[1] Faculty of Applied Design and Engineering, Swansea Metropolitan University; Swansea, UK; Phone: +44(0)1792 481000; e-mail: stephen.mosey@smu.ac.uk, peter.charlton@smu.ac.uk, ian.wells@smu.ac.uk

Abstract

In B-mode imaging, lateral resolution is impeded by the size and shape of the ultrasound beam used to create the image. For improved lateral resolution, a focussing method that utilises a beam model calculated using the Fraunhofer far field approximations to enhance the Synthetic Aperture Focussing Technique (SAFT) is proposed. The Beam Model Weighted Synthetic Aperture Focussing Technique (BMW-SAFT) method uses an approximation of the beam model to weight the focussing algorithm and adjust the aperture size based on distance from the transducer. Through application to simulated data the method is compared with the conventional SAFT, where the proposed algorithm is found to provide significant improvements over the conventional SAFT methods.

Keywords: ultrasound, synthetic aperture focussing (SAFT), B-Scan, phased array, linear array

1 Introduction

The objective of this paper is to investigate the synthetic aperture focusing technique, its application to ultrasound, and to develop and evaluate an enhanced algorithm to improve its performance. The SAFT suffers from two major downfalls; firstly, the inability to focus at all depths evenly; and secondly, the presence of artifacts within the focused image generated as a side effect of the algorithm. The BMW-SAFT algorithm uses the Fraunhofer approximation to model the far field of the ultrasound beam, which is then used to determine the size of the aperture and the weights applied across the aperture during the focusing process.

2 Synthetic Aperture Focussing Technique

2.1 Basic Principles

The SAFT uses a series of delay and average operations on each pixel in an image to focus the image. The amount of delay applied to each pixel is dependent on which area is currently being focussed and how far away the pixel is from that area. Signals received by the transducer may not have come from indications directly below it; this is due to reflectors laying within the beam spread of the transducer creating indications in the signal as illustrated in figure 1. These defect indications are then plotted at the apparent depth beneath the transducer's current position. As the transducer approaches the defect, the indications in the image are plotted at greater amplitudes nearer the actual depth of the defect. As the transducer moves away from the defect, the defect's apparent depth increases while the amplitude of the signal drops. This has the effect of adding parabolic tails to the edges of indications within the B-Scan image. Using the SAFT method, this distortion of the indication can be reduced somewhat.

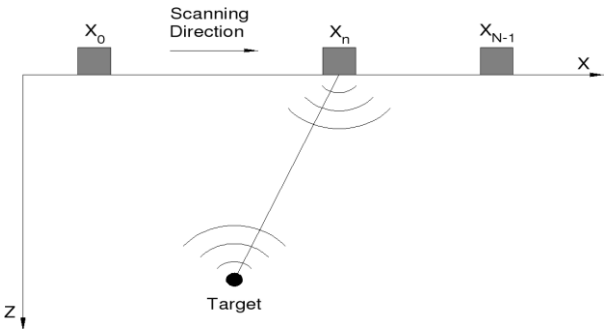

Figure 1. Image Formation [1].

2.2 Conventional SAFT

The conventional SAFT algorithm uses a series of delay and sum procedures to geometrically focus the image. The amount of delay added to each signal is found using the Pythagorean sum of the distances between the elements in the image being considered for the point currently being focussed and the transducer. These delays mimic the typical hyperbolic shape of an indication from a point source in an ultrasound B-mode image, points along this parabola are averaged and the resulting value is placed in the new, focussed image at the apex of the parabola. The apparent depth of the indication, $T_{x,z}$, viewed by a transducer at a location $X_n$is the Pythagorean sum of the distances between the transducer and the indication, as expressed in equation 1.

$$T_{x,z}{}' = \sqrt{T_z{}^2 + (T_x - X_n)^2} \quad \text{.....(1)}$$

This forms the heart of the geometric model of the SAFT algorithm. It is used to calculate the shape of the parabola used to locate relevant pixels within the image to sum. The algorithm for the conventional SAFT is described by equation 2.

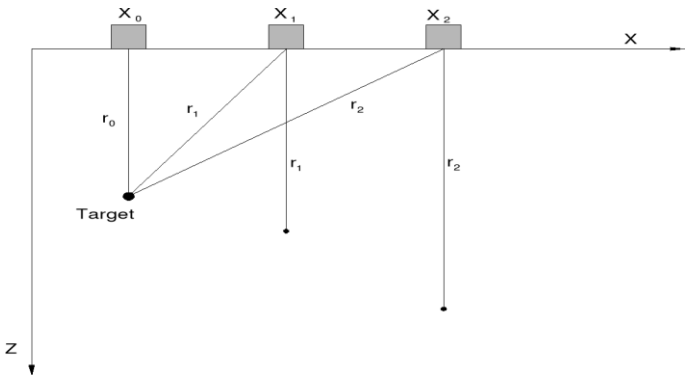

Figure 2. Depth of indication changing with transducer position.

$$P'_{x,z} = \frac{1}{m}\sum_{i=-\frac{m}{2}}^{\frac{m}{2}} P_{x+i,\sqrt{z^2+i^2}} \quad \text{.....(2)}$$

Where *P'* is the point located at *x*, *z* and *m* is the aperture width. The algorithm seeks to find all possible points in the unfocussed image that *could* have indications contributing to the point, $P_{x,z}$, and average them across an aperture *m* to form a new focussed point, $P'_{x,z}$ within a new image.

2.3 Beam Model Weighted SAFT

In the standard SAFT model, for a fixed aperture size the level of focus applied to the image degrades linearly with depth. This is due to the divergence of the ultrasound beam. As the focal point gets further and further away from the transducer, the beam becomes wider than the selected aperture, this means the algorithm will be missing contributions from pixels outside the aperture containing valid data relating to the current focus point. Conversely, near the surface the aperture is wider than the ultrasound beam, thus points that would not have contributed would be wrongly included. This effect can be seen in SAFT processed images, consider an image with two identically sized indications, as in figure 3, one near the transducer, the other much further away. With a conventional SAFT algorithm, the indication further away from the transducer will appear larger and less focused than an indication at a point where the beam width is equal to the aperture width. If such an aperture is chosen that the indication further away is brought into sharp focus, the indication near the transducer will now appear lower in amplitude than it otherwise should be, and will also show artefacts due to the erroneous points included in the summing operation that lie outside the beam width at that depth.

The work of Burch and Burton and others [2, 3, 4, 5], seem to be seeking to find a weighting function to modify the SAFT algorithm to allow a sharp focus be applied to the entire image while minimising artefacts generated by the focussing algorithm itself. Burch and Burton used a Gaussian function as a weighting applied to the standard SAFT algorithm. While others have used Hamming windows, Hanning windows, and cosine functions as weighting functions; all of which could be said to somewhat resemble the lateral amplitude profile at some depth for the beam model of an ultrasound transducer. It seems only logical that the weighting function applied to the algorithm should closely resemble the beam model of the ultrasound transducer used. It follows that the aperture width should also vary with depth, as the focussing performance of the standard SAFT algorithm using a rectangular aperture, can be considered to vary linearly with depth.

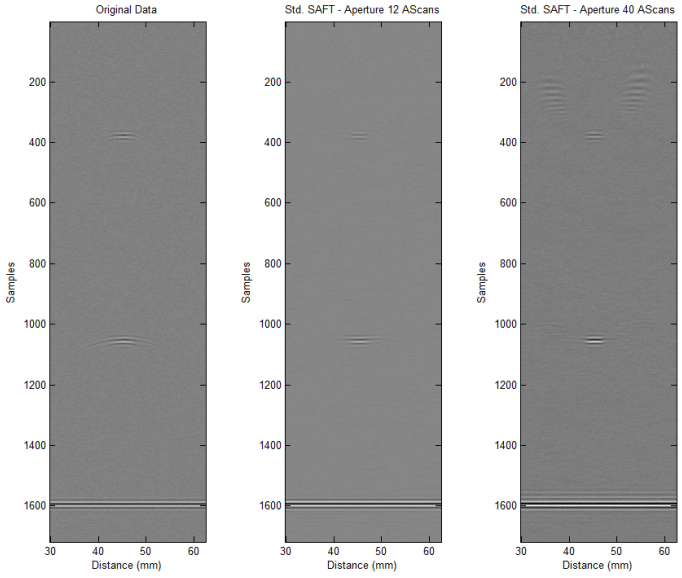

Figure 3. Effect of aperture width on focal depth for the standard SAFT Model. Left: Original image, Centre: aperture width chosen to focus top indication, Right: aperture width chosen to focus bottom indication.

Consider again two reflectors that share the same *X* coordinate within an image, as shown in figure 4. If they are to be imaged using a transducer placed on the surface such that the reflector nearer the surface (reflector 1) falls outside the beam spread of the transducer, while

the reflector further away (reflector 2) lies within the ultrasound beam; the transducer will only receive signals from the reflector 2, and not from reflector 1. If the image acquired from this were to be processed by the standard SAFT algorithm, using a rectangular aperture chosen such that neither reflector 1 nor reflector 2 were grossly out of focus. While focussing at the *Z* coordinates above reflector 1 and above reflector 2, if too many points are included in the summing operation, a large proportion of the information contained in the echo from reflector beneath would be included, creating a large artefact or pre-echo. From this, it can be deduced that the aperture width required to focus the entire image correctly is related to the divergence of the ultrasound beam.

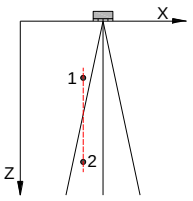

Figure 4. Two reflectors beneath a transducer sharing the same X coordinate, one inside and one outside the ultrasound beam.

By including information about the ultrasonic beam used to create a data set, a more accurate focussing method can be applied. To generate information about the beam profile of the transducer, a Fraunhofer diffraction model is employed. The geometric model of the standard SAFT algorithm is still used to calculate the positions of the pixel points for the delay and sum process. Each pixel in the delay and sum operation is weighted based upon the amplitude of the transducer beam at that point. This is illustrated in equation 3, the first part of this equation is identical to that of the standard SAFT model, this is the geometric model of SAFT; the second part of this equation provides the weighting functions from the transducer model (equation 4).

$$P'_{x,z} = \frac{1}{m_z} \sum_{i=-m_z/2}^{m_z/2} P_{x+i,\sqrt{i^2+z^2}} \cdot W_{i,\sqrt{i^2+z^2}} \quad \text{.....(3)}$$

Where $m_z = \#(W_z \geq Th)$ is the number of values in *W* at a depth *z* that are equal to, or greater than a threshold *Th*. This threshold can be based upon a desired beam angle, as shown in figure 5. The aperture size is calculated based upon the current depth of focus of the algorithm; this leads to a variable loss of data at each end of the scan, as illustrated in figure 6, where θ illustrates the extremity of the ultrasound beam used to calculate the weights. However, this can be compensated for by capturing more data than would otherwise be required.

$$W_{x,z} = \left\{ \left(a_0 w \frac{\sin \alpha}{\alpha} \right) \left(\frac{\sin(N\beta)}{\sin(\beta)} \right) \right\}^2 \quad \text{.....(4)}$$

Where a_0 is the peak amplitude, *w* is the element width, $\alpha = \frac{kw \sin \theta}{2}$, and $\beta = \frac{kd \sin \theta}{2}$, $k = \frac{2\pi}{\lambda}$, $\theta = \tan^1 \frac{x}{z}$, *d* is the element pitch, *N* is the number of elements in the transducer, *x* and *z* are the lateral and axial distances from the transducer face to the point where the intensity is to be found.

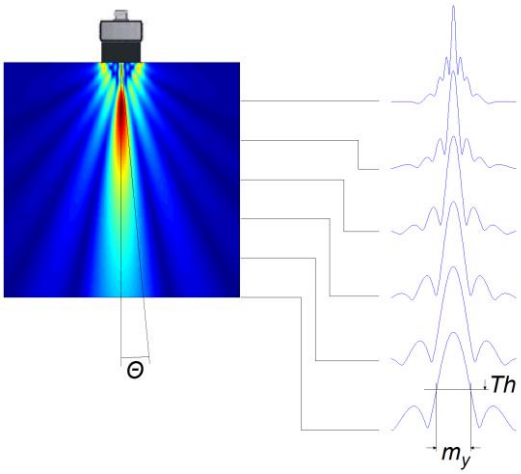

Figure 5. Threshold based on a beam angle.

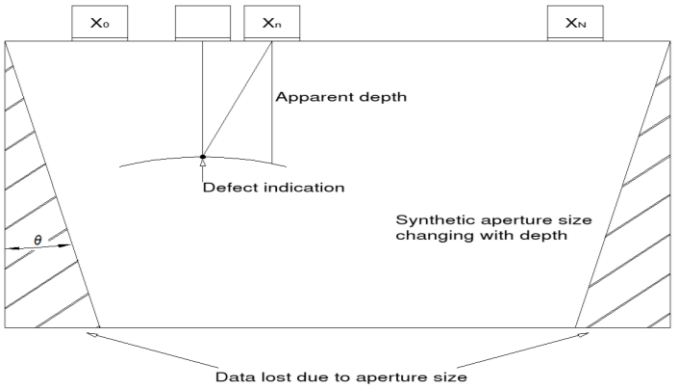

Figure 6. Data loss caused by varying aperture size.

3 Experimental Comparison

The experimental comparison reported here consists of simulations of three different slot widths at three different depths. The validated simulation method utilized has been described previously [6]. Indications were placed at 10mm, 20mm and 30mm from the surface of the material. Indication lengths were chosen to challenge the algorithm as much as possible; therefore indication lengths were chosen to be less than the beam width, equal to the beam width and larger than the -6dB beam width. Using an aperture size of four elements, the -6dB beam edge is at ±12° from the normal. This allows for the slot lengths to be calculated, using half the beam width, the whole beam and one and a half times the beam width. The simulated slot dimensions are listed in Table 1.

Table 1. Simulated slot dimensions.

Simulation	Slot depth from material surface (mm)	Beam width at slot depth (mm)	Slot width (mm)
1	10	4.251	2.126
2	20	8.502	8.502
3	30	12.753	19.130

To assess the performance of the proposed BMW-SAFT algorithm, the simulated images were processed with both the standard SAFT algorithm and the BMW-SAFT algorithm. Cross sectional amplitudes for the simulated indications were plotted for the raw data from the

simulations, along with the results from both the SAFT and BMW-SAFT algorithms. These graphs allow comparisons of indication size, and focussing artefacts.

From the simulation results shown in Figures 7 to 9, it can be seen that in the standard SAFT processed images all contain an element of algorithm induced artifacts; these are highlighted as lower amplitude peaks either side of the main peak in the bottom centre graph in the relevant figures.

The images processed using the proposed BMW-SAFT method all show very low level artifacts either side of the main peaks, typically <-26dB, this is far better than the artifact level of the standard SAFT processed images which is typically -14dB. The proposed BMW-SAFT algorithm also shows results for planar type indications, such as the horizontal slots simulated here, with flatter, more uniform peaks that show a much better level of symmetry than the same results as the standard SAFT algorithm.

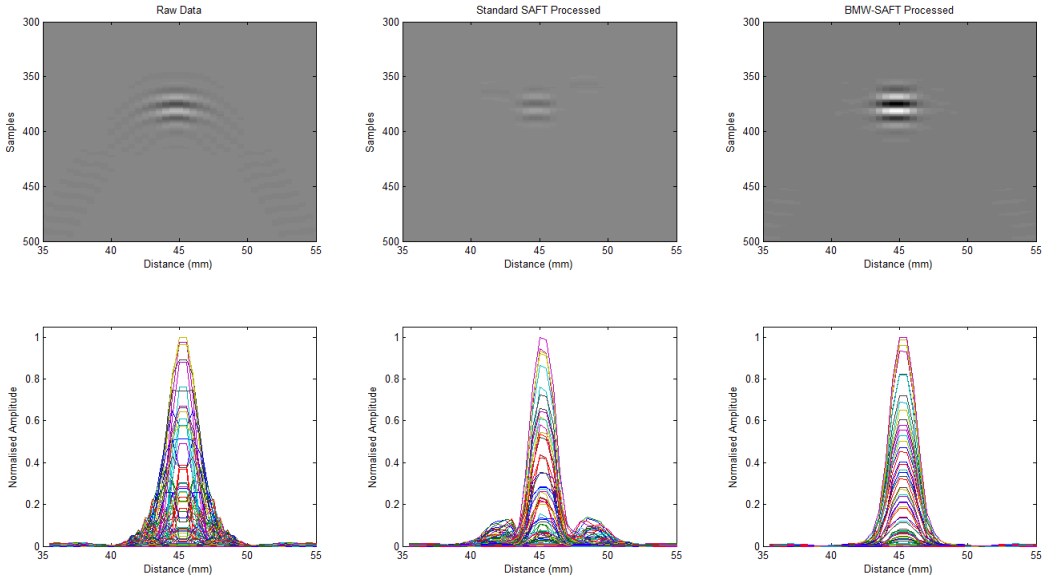

Figure 7. Raw and processed images for a 2.126mm wide slot at a depth of 10mm.

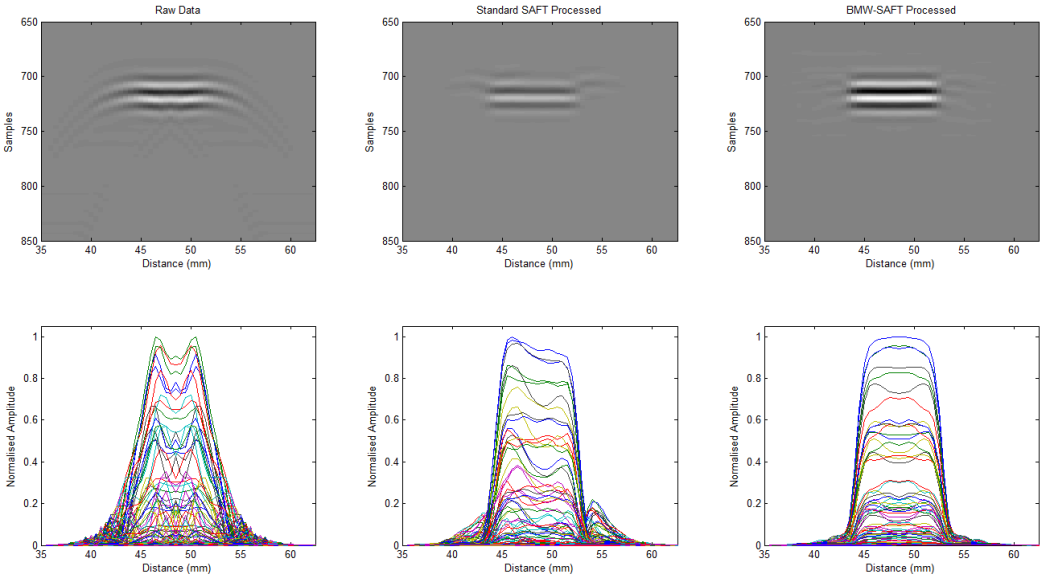

Figure 8. Raw and processed images for an 8.502mm wide slot at a depth of 20mm.

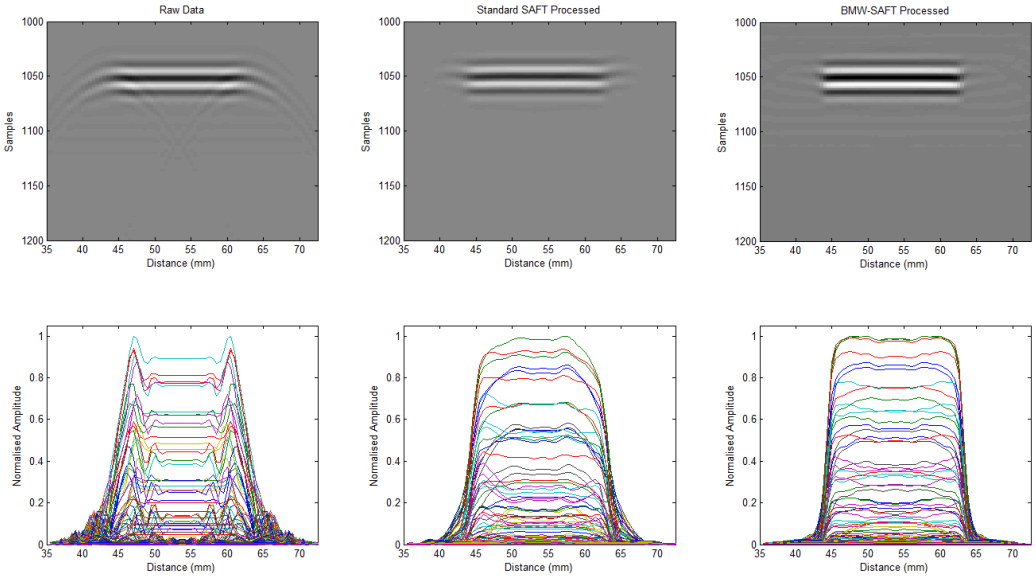

Figure 9. Raw and processed images for a 19.130mm wide slot at a depth of 30mm.

4 Conclusions

While several variations of the SAFT algorithm have been proposed by many, the BMW-SAFT algorithm includes information about the ultrasonic beam used to create the image; and adjusts the aperture size according to the width of the beam through the range of depths required. This enables the algorithm to focus the entire image without any degradation in performance with depth, as can be seen with the standard SAFT algorithm. The linearly changing aperture size combined with the lateral amplitude distribution from the beam model ensures algorithm generated artefacts are minimised across the entire image. The far field approximation used in the algorithm is a valid choice of beam model as the transmit aperture size for the transducer would be selected such that the near field of the active aperture would end far above the expected depth of any defects within the component under test.

Using modern computers, the increase in complexity of the algorithm is barely noticeable. The beam model used to create the weighting factors, and aperture size variations, uses a 1D linear array of rectangular elements; but this could easily be tailored to suit any transducer configuration. A linearly increasing loss of data caused by the aperture size variations near the edges of images processed with the BMW-SAFT algorithm would need to be compensated for by acquiring extra data at the start and end of the scan.

References

1. F. Lingvall, T. Olofsson, T. Stepinski, ‘Synthetic Aperture Imaging Using Sources With Finite Aperture: Deconvolution of the Spatial Impulse Response’, The Journal of Acoustical Society of America, pp 225-234, July 2003.
2. S. F. Burch, J. T. Burton, ‘Ultrasonic Synthetic Aperture Focusing Using Planar Pulse-Echo Transducers’, Ultrasonics, Vol 22, No 6, pp 270-274, November 1984.
3. J. T. Ylitalo, H. Ermet, ‘Ultrasound Synthetic Aperture Imaging: Monostatic Approach’, IEEE Transactions on Ultrasonics, Ferroelectrics and Frequency Control, Vol 41, No 3, pp 333-339, May 1994.

4. W. Masri, M. Mina, S. S. Udpa, L. Udpa, T. Xue, W. Lord, ‘Synthetic Aperture Focussing Techniques Applied in the Near Field of a Focused Transducer’, IEEE Ultrasonics Symposium, pp 783-786, November 1995.
5. C. H. Frazier, W. D. O'Brien, ‘Synthetic Aperture Techniques with a Virtual Source Element’, IEEE Transactions on Ultrasonics, Ferroelectrics and Frequency Control, Vol 45, No 1, pp 196-207, January 1998.
6. Mosey S.A.,Charlton P.C., Wells I., ‘Resolution enhancement of ultrasonic B-mode images’, Insight, Vol 55, No 2, February 2013.